Low-Frequency Equatorial Waves in Vertically Sheared Zonal Flow. Part II: Unstable Waves

XIAOSU XIE* AND BIN WANG

Department of Meteorology, University of Hawaii, Honolulu, Hawaii

(Manuscript received 31 December 1995, in final form 4 June 1996)

ABSTRACT

The stability of equatorial Rossby waves in the presence of mean flow vertical shear and moisture convergence-induced heating is investigated with a primitive equation model on an equatorial β plane.

A vertical shear alone can destabilize equatorial Rossby waves by feeding mean flow available potential energy to the waves. This energy transfer necessitates unstable waves' constant phase lines tilt both horizontally (eastward with latitude) and vertically (against the shear). The preferred most unstable wavelength increases with increasing vertical shear and with decreasing heating intensity, ranging typically from 3000 to 5000 km. The instability strongly depends on meridional variation of the vertical shear. A broader meridional extent of the shear allows a faster growth and a less-trapped meridional structure. When the shear is asymmetric relative to the equator, the unstable Rossby wave is constrained to the hemisphere where the shear is prominent. Without boundary layer friction the Rossby wave instability does not depend on the sign of the vertical shear, whereas in the presence of the boundary layer, the moist Rossby wave instability is remarkably enhanced (suppressed) by easterly (westerly) vertical shears. This results from the fact that an easterly shear confines the wave to the lower level, generating a stronger Ekman-pumping-induced heating and an enhanced meridional heat flux, both of which reinforce the instability.

The moist baroclinic instability is a mechanism by which westward propagating rotational waves (Rossby and Yanai waves) can be destabilized, whereas Kelvin waves cannot. This is because the transfer of mean potential energy to eddy requires significant magnitude of barotropic motion. The latter is a modified Rossby wave and can be resonantly excited only by the westward propagating rotational waves. The common features and differences of the equatorial Rossby wave instability and midlatitude baroclinic instability, as well as the implications of the results are discussed.

1. Introduction

In Part I (Wang and Xie 1996, hereafter WX96) of this paper, the mechanism by which a vertically sheared zonal flow affects the structure and propagation of equatorial waves was examined. It was shown that a moderate vertical shear has little impact on equatorial Kelvin waves but remarkable effects on equatorial Rossby and westward propagating Yanai waves. This is due to the fact that modification of wave properties depends on the magnitude of the barotropic motion component. The barotropic component of the equatorial wave motion is a modified Rossby mode and can be resonantly excited only by westward propagating internal waves. It is not clear whether this selective excitation of barotropic motion may also affect the instability of the equatorial waves. WX96 also found that in the Tropics a westerly shear favors trapping of Rossby waves in the upper troposphere, while an easterly shear confines Rossby waves in the lower troposphere. The different effects of vertical shears on wave structure are expected to have a major impact on the strength of the boundary layer moisture convergence. The latter may in turn influence the Rossby wave through organized convective heating, changing the wave stability. In this paper, we will further investigate the instability of the equatorial waves and address the issue of how a vertically sheared zonal flow and boundary layer moisture convergence-induced heating destabilize equatorial waves.

The present study is also motivated by the need to interpret the nature of the observed low-frequency westward propagating disturbances, which are reproducible in numerical models as well. Whereas the westward propagation is sometimes episodic and the intensity is relatively weak, it is a prevailing mode in off-equatorial monsoon domain (along 10°–20°N from 170°E to 110°E) in August and September. The westward propagating disturbances were found over the South Asia and the western North Pacific regions on

* Current affiliation: Jet Propulsion Laboratory, California Institute of Technology, Pasadena, California.

Corresponding author address: Dr. Bin Wang, Department of Meteorology, University of Hawaii, 2525 Correa Road, Honolulu, HI 96822.

10–20-day and 30-day timescales (e.g., Murakami 1980; Cadet 1983; Nitta 1987; Wang and Rui 1990a). They exhibit a typical westward phase speed of a few meters per second and a zonal scale (one-quarter of wavelength) of the equatorial Rossby radius of deformation (1000–1500 km). The behavior of the synoptic (about 8–9 day) westward-propagating waves with a typical wavelength of 4000 km and a speed of 5 m s^{-1} were documented in detail by Lau and Lau (1990). These disturbances are characterized by an eastward tilt with latitude of the constant phase lines and by low-level cyclonic (anticyclonic) vorticity accompanying by enhanced (suppressed) convection. In the troposphere, their troughs and ridges tilt eastward with height, against the direction of the vertical shear. These observed features call for explanations.

Whereas observations show a strong evidence of the linkage between the westward-moving low-frequency modes and the South Asian summer monsoon circulation, theoretical explanation of the phenomenon has been lacking. Based on their numerical experiments, Lau and Peng (1990) suggested that an equatorial intraseasonal mode interacting with the Asian monsoon flows can generate westward-moving synoptic disturbances in monsoon regions. They interpreted these disturbances as resulting from quasigeostrophic baroclinic instability of the monsoon flows. Zhang and Geller (1994) investigated the impacts of vertical shears on CISK waves. Their analysis for the Rossby waves is also based on a quasigeostrophic β-plane model. Since the tropical atmospheric motions consist of a significant ageostrophic component, a primitive equation model is more relevant for study of equatorial Rossby waves that have large-amplitude pressure fluctuation at one Rossby radius of deformation (10°–15° latitude) and strong zonal wind along the equator. Kuo (1978) studied combined barotropic and baroclinic instability in the Tropics and concluded that the tropical disturbances develop primarily through barotropic instability whereas baroclinic instability has trivial impact on the growth rate. His model atmosphere is free of heating and in a regime in which the barotropic instability is dominant. The condensational heating, however, plays an essential role in the tropical wave dynamics and tropical circulation. Static stability can be substantially reduced by latent heating, and thus critical vertical wind shear required for baroclinic instability can be much smaller than its adiabatic counterpart.

The present analysis will address some interesting questions regarding the equatorial wave instability. For instance, why does the Northern Hemisphere summer monsoon circulation favor the development of the westward propagating disturbances rather than the eastward propagating equatorial Kelvin waves? In particular, what roles does the monsoon easterly vertical shear play in the development of the low-frequency equatorial waves? If the westward propagating disturbances are interpreted as equatorial Rossby waves, how are the equatorial Rossby waves destabilized by a vertical wind shear? What is the fundamental difference between the tropical Rossby wave instability and the midlatitude baroclinic instability? The vertical easterly shears in the boreal summer monsoon region exhibit strong asymmetry with respect to the equator. How does the latitudinal variation of the vertical shear affect the equatorial Rossby wave instability? These questions are the targets of the present study.

2. The model

The dynamic model used in this study is basically the same as that used in Part I (WX96). It consists of a two-level representation of baroclinic structure of the low-frequency motion. Details of the derivation of model equations can be found in Part I.

For convenience of the analysis and physical understanding we define a barotropic and a baroclinic mode by

$$u_+ = \frac{1}{2}(u_1 + u_2), \quad v_+ = \frac{1}{2}(v_1 + v_2),$$

$$\phi_+ = \frac{1}{2}(\phi_1 + \phi_2), \tag{2.1a}$$

$$u_- = \frac{1}{2}(u_1 - u_2), \quad v_- = \frac{1}{2}(v_1 - v_2),$$

$$\phi_- = \frac{1}{2}(\phi_1 - \phi_2). \tag{2.1b}$$

The nondimensional governing equations for hydrostatic, perturbation motions with a mean zonal wind varying with height on an equatorial β plane can be written as (WX96)

$$\frac{Du_+}{Dt} - yv_+ + \frac{\partial \phi_+}{\partial x} = -2U_T\frac{\partial u_-}{\partial x} - U_T\frac{\partial v_-}{\partial y} - U_T' v_- - \epsilon u_+, \tag{2.2a}$$

$$\frac{Dv_+}{Dt} + yu_+ + \frac{\partial \phi_+}{\partial y} = -U_T\frac{\partial v_-}{\partial x} - \epsilon v_+, \tag{2.2b}$$

$$\frac{\partial u_+}{\partial x} + \frac{\partial v_+}{\partial y} = 0, \tag{2.2c}$$

$$\frac{Du_-}{Dt} - yv_- + \frac{\partial \phi_-}{\partial x} = -U_T\frac{\partial u_+}{\partial x} - U_T' v_+ - \epsilon u_-, \tag{2.2d}$$

$$\frac{Dv_-}{Dt} + yu_- + \frac{\partial \phi_-}{\partial y} = -U_T\frac{\partial v_+}{\partial x} - \epsilon v_-, \tag{2.2e}$$

$$\frac{D\phi_-}{Dt} + (1 - I)\left(\frac{\partial u_-}{\partial x} + \frac{\partial v_-}{\partial y}\right) = yU_T v_+ - \epsilon_p \phi_-, \tag{2.2f}$$

where ϵ and ϵ_p are the Rayleigh friction and Newtonian cooling coefficients, respectively; and

$$\frac{D}{Dt} \equiv \frac{\partial}{\partial t} + \bar{U}\frac{\partial}{\partial x}, \tag{2.3a}$$

$$\bar{U} = \frac{1}{2}(\bar{u}_1 + \bar{u}_2), \quad U_T = \frac{1}{2}(\bar{u}_1 - \bar{u}_2), \tag{2.3b}$$

$$U_T' \equiv \frac{dU_T}{dy}. \tag{2.3c}$$

Because the barotropic mode is nondivergent under rigid-lid vertical boundary conditions, it can be described by a barotropic streamfunction ψ

$$u_+ = -\frac{\partial \psi}{\partial y}, \quad v_+ = \frac{\partial \psi}{\partial x}. \tag{2.4}$$

The barotropic motion is then governed by a nondivergent vorticity equation

$$\left(\frac{D}{Dt} + \epsilon\right)\nabla^2\psi + \frac{\partial \psi}{\partial x} = -U_T\left[\frac{\partial}{\partial x}\left(\frac{\partial v_-}{\partial x} - \frac{\partial u_-}{\partial y}\right) - \frac{\partial}{\partial y}\left(\frac{\partial u_-}{\partial x} + \frac{\partial v_-}{\partial y}\right)\right] + 2U_T'\left(\frac{\partial u_-}{\partial x} + \frac{\partial v_-}{\partial y}\right) + U_T'' v_-, \tag{2.5}$$

where

$$U_T'' \equiv \frac{d^2U_T}{dy^2}. \tag{2.6}$$

The nondimensional heating coefficient I represents a condensational heating rate normalized by adiabatic cooling rate due to the vertical motion at the middle troposphere. Typical values of I can be estimated based on the moisture content and mean static stability of the basic state (Wang 1988). With normal conditions in the tropical atmosphere, I is less than unity. Here, $\bar{U}$ and U_T denote vertical mean and vertical shear of the mean zonal flow, respectively. Equation (2.5) describes the barotropic mode, which is a Rossby wave interacting with the internal (baroclinic) mode in the presence of vertical shear. Equations (2.2d–f) are shallow-water equations applied to the lowest internal mode, which is modified by the barotropic mode and vertical shear.

The vertical pressure velocity was assumed to vanish at the upper and lower boundaries in the absence of boundary layer effects. When the boundary layer frictional convergence is included, the model equations and vertical boundary conditions are modified, which will be discussed in section 7. At the lateral boundaries $y = y_b$ and $-y_b$, the perturbation meridional wind and the meridional derivatives of perturbation geopotential and zonal wind are assumed to vanish. This boundary condition is adequate only for trapped equatorial waves. In the present study, the half-width of the equatorial β channel is chosen to be 5.0 and the increment of y is 0.1. The high resolution in y and large half-width of the channel are necessary in order to get converging solutions. Zonally propagating normal mode solutions are assumed. Equations in terms of the y-dependent amplitudes along with the meridional boundary conditions are solved by a matrix inversion to obtain characteristic structure, growth rate, and phase speed of the normal mode.

The validity of the equatorial β-plane approximation is verified by parallel computations using a spherical coordinate model (see appendix in WX96). It shows that results are basically similar to those using the equatorial β-plane model, provided that the lateral boundaries are about four Rossby radii of deformation away from the equator.

3. Energetics

To analyze energy sources for possible instability, we derive a set of energy equations. A barotropic kinetic energy equation can be obtained by adding (2.2a) multiplied by u_+ and (2.2b) multiplied by v_+ and then averaging the resulting equation from $y = -y_b$ to $y = y_b$ and over a zonal wavelength. In a similar manner, a baroclinic kinetic energy equation can be obtained from (2.2d) and (2.2e). Finally, an equation for baroclinic available potential energy can be derived by multiplying (2.2f) by ϕ_- and taking horizontal average. These equations are

$$\frac{\partial K_+'}{\partial t} = \langle K_-', K_+' \rangle + \mathrm{GK}_+ - 2\epsilon K_+', \tag{3.1}$$

$$\frac{\partial K_-'}{\partial t} = \langle P_-', K_-' \rangle - \langle K_-', K_+' \rangle + \mathrm{GK}_- - 2\epsilon K_-', \tag{3.2}$$

$$\frac{\partial P_-'}{\partial t} = -(1 - I)\langle P_-', K_-' \rangle + \langle \bar{P}, P' \rangle - 2\epsilon_p P_-', \tag{3.3}$$

where

$$K_-' = \frac{1}{2}(\overline{u_-^2 + v_-^2}), \tag{3.4a}$$

$$K_+' = \frac{1}{2}(\overline{u_+^2 + v_+^2}), \tag{3.4b}$$

$$P_-' = \frac{1}{2}\overline{\phi_-^2}, \tag{3.4c}$$

$$\langle P_-', K_-' \rangle = \overline{\phi_-\left(\frac{\partial u_-}{\partial x} + \frac{\partial v_-}{\partial y}\right)}, \tag{3.4d}$$

$$\langle K_-', K_+' \rangle = -\overline{U_T\left(u_+\frac{\partial u_-}{\partial x} + v_+\frac{\partial v_-}{\partial x}\right)}, \tag{3.4e}$$

$$\langle \bar{P}, P'_- \rangle = \overline{U_T y v_+ \phi_-}, \tag{3.4f}$$

$$\mathrm{GK}_+ = -\overline{U_T u_+ \left(\frac{\partial u_-}{\partial x} + \frac{\partial v_-}{\partial y} \right)} - \overline{U'_T u_+ v_-}, \tag{3.4g}$$

$$\mathrm{GK}_- = -\overline{U'_T u_- v_+}, \tag{3.4h}$$

where the overbar in the right-hand sides of (3.4) represents a horizontal average. Here, K'_+, K'_-, and P'_- denote horizontal mean eddy barotropic kinetic energy, baroclinic kinetic energy, and available potential energy, respectively. Here, $\langle P'_-, K'_- \rangle$ measures conversion from the eddy available potential energy to the eddy baroclinic kinetic energy, which is proportional to the covariance between temperature and wave-induced convergence. The $\langle K'_-, K'_+ \rangle$ is conversion from eddy baroclinic kinetic energy to the barotropic kinetic energy, which depends on vertical shear. The vertical shear acts as a coupling factor between baroclinic and barotropic motions. The $\langle \bar{P}, P'_- \rangle$ is conversion from the mean flow potential energy to eddy available potential energy, and it is proportional to eddy meridional heat flux and vertical shear. The $I\langle P'_-, K'_- \rangle$ denotes generation of eddy available potential energy resulting from condensational heating associated with wave-induced moisture convergence. The term GK_+ represents generation of eddy barotropic kinetic energy resulting from the coupling of the two modes by vertical shear, without which the barotropic motion cannot be excited by an internal heating. The term GK_- is the generation rate of eddy baroclinic kinetic energy due to meridional variation of the vertical shear of the mean zonal flow. It is negligibly small. The vertical shear of mean zonal flow is a potential source of instability for perturbations. The role of condensational heating associated with interior wave divergent motion is to reduce the effective static stability of the basic state. Without vertical shear there is no net generation of eddy available potential energy, because parameter I is usually less than unity.

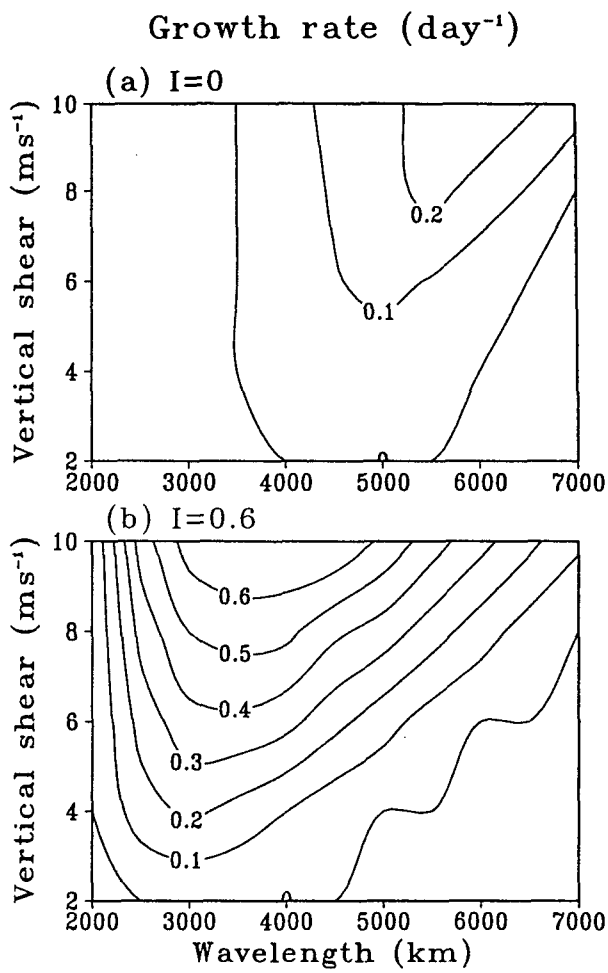

FIG. 1. Growth rate for the Rossby wave (n = 1) as a function of vertical shear and wavelength with nondimensional heating parameter (a) I = 0 and (b) I = 0.6.

4. Destabilization of equatorial Rossby waves by vertical shear

In this section, we elucidate how a vertical shear destabilizes equatorial Rossby waves. Consider first a zonal flow with a constant vertical shear. In Part I, it was shown that for the same magnitude of the shear, eigenvalues are invariant with respect to the sign of the shear. This is also the case for unstable waves. It thus suffices to discuss only easterly shears in this section. In the following analysis, the Rayleigh friction and Newtonian cooling are neglected.

The growth rate of n = 1 Rossby wave (n is an index for the meridional modes) increases markedly with increasing strength of vertical shear (Fig. 1) due to enhanced available potential energy transfer from the mean flow to waves. The latent heating also greatly enhances the instability (Fig. 1b) by reducing the static stability of the basic state. For a fixed vertical shear and heating intensity, the instability has a preferred wavelength from 3000 to 5500 km corresponding to the largest growth rate. The instability does not occur on planetary or very short scales. The most unstable wavelength shows a weak tendency to increase with increasing magnitude of vertical shear. The heating leads to a shorter most unstable wavelength. For nondimensional heating parameter I = 0.6 and vertical shear $U_T = -6$ m s^{-1}, the most unstable wavelength is 3500 km with an e-folding time of 2.6 days for the inviscid growth rate and a westward phase speed of 2.8 m s^{-1} without vertical mean zonal flow ($\bar{U} = 0$). The westward phase speed is reduced as latent heating increases or horizontal scale decreases (figure not shown).

The horizontal structure of unstable Rossby waves differs considerably from that of stable Rossby waves.

A stable long Rossby wave consists of a trapped baroclinic mode and an "emanated" barotropic mode, which has geopotential maximum at midlatitudes (WX96). Both the baroclinic and barotropic modes of the unstable Rossby wave remain trapped in the Tropics, displaying a single extreme in each hemisphere in the geopotential (Fig. 2). The maximum geopotential perturbation of the barotropic mode is located approximately at $y = \pm 1.5$, and the corresponding baroclinic counterpart is located slightly poleward. The magnitudes of the two vertical modes are comparable. The equatorial zonal winds associated with an unstable wave are much weaker than those associated with a stable wave, but meridional winds away from the equator are much stronger. The temperature perturbation of unstable waves is less trapped to the equator compared to that of stable waves.

Another distinct feature of an unstable Rossby wave is that the constant phase lines tilt eastward with latitude for both the baroclinic and barotropic modes. This contrasts the structure of the stable long Rossby waves whose constant phase lines have no meridional tilt for both modes (WX96).

From an energetic point of view, the horizontal structure of the unstable Rossby wave is constructive for transferring available potential energy from mean flow to eddies. The conversion rate ($\langle \bar{P}, P'_- \rangle = U_T \overline{yv_+\phi_-}$) is proportional to the Coriolis parameter (or latitude),

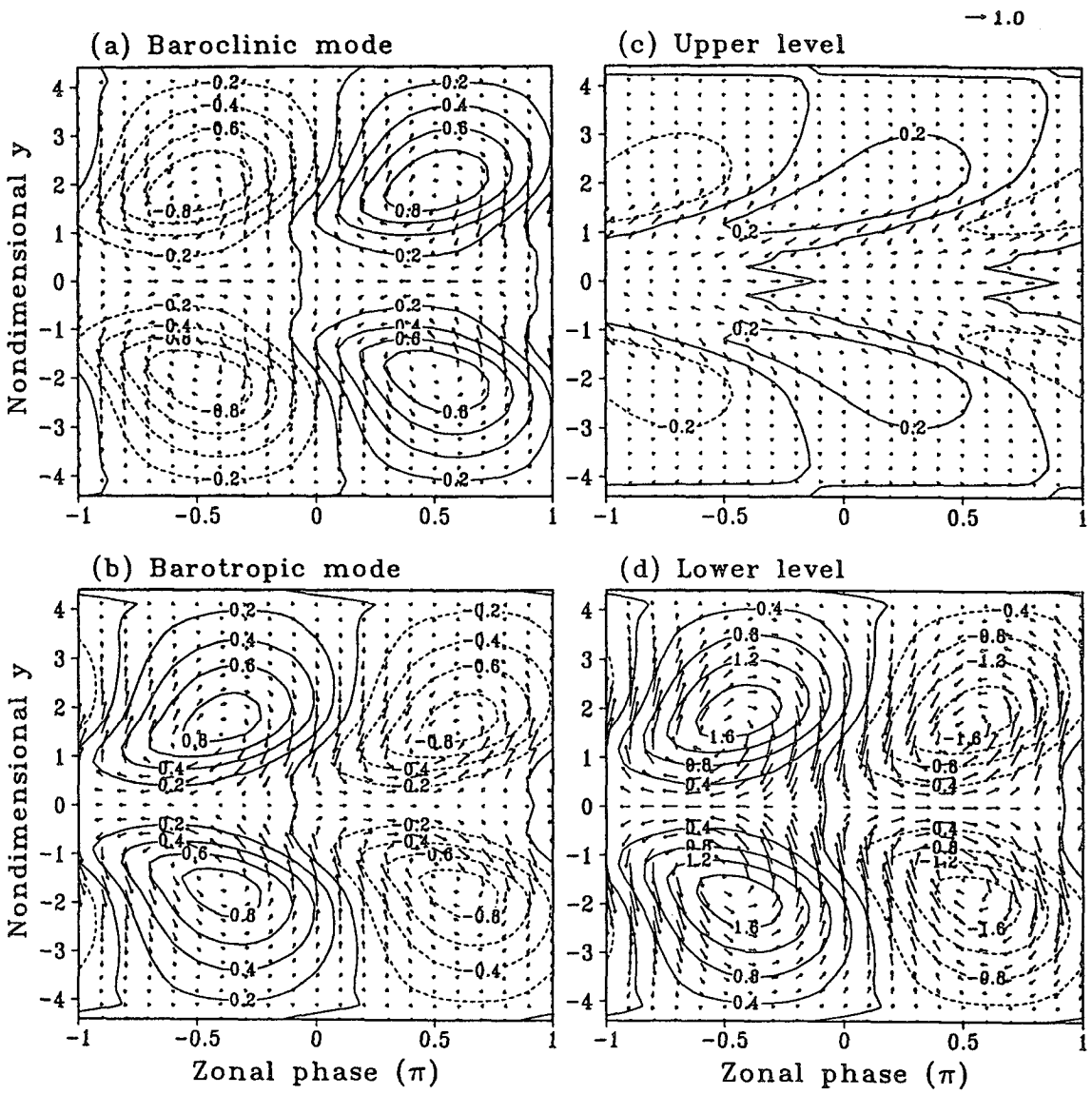

FIG. 2. Geopotential and flow patterns of the (a) baroclinic mode, (b) barotropic mode, (c) upper level, and (d) lower level for the $n = 1$ Rossby wave with a wavelength of 5000 km for $U_T = -6$ m s^{-1} and $I = 0.8$.

vertical shear, and the meridional heat flux by barotropic wind. An effective conversion demands sufficiently large Coriolis parameter. It also requires large-magnitude temperature and barotropic meridional wind be located at about the same latitudes so that their covariance maximizes. The latter is a key for instability. In a stable wave case, the baroclinic and barotropic modes are 180° out of phase in an easterly shear and precisely in phase in a westerly shear (WX96). Consequently, the temperature field is precisely in quadrature with the barotropic meridional wind and the integrated covariance over one wavelength is zero (figure not shown). As such, there is no net conversion from the mean potential energy to eddies. For an unstable Rossby wave, on the other hand, both the baroclinic and barotropic modes are approximately 180° out of phase in the vicinity of the equator in an easterly shear (Fig. 2). Away from the equator, however, the phases of both the vertical modes, especially the barotropic mode, tilt eastward with increasing latitude. As such, v_+ and ϕ_- are not in a perfect quadrature relationship, thus zonal average of the covariance between v_+ and ϕ_- does not vanish (Fig. 3), yielding a conversion of available potential energy from mean flow to waves in both the easterly and westerly shears.

In general, the rate of conversion of mean to eddy available potential energy determines the growth rate of adiabatic unstable Rossby waves. It is worthwhile to further discuss the relationship between the wave growth and horizontal structure. Assuming that barotropic meridional wind v_+ lags temperature perturbation ϕ_- by a phase angle α. It can be shown that the transfer of available potential energy from mean flow to eddies requires $U_T \cos\alpha > 0$. In an easterly shear ($U_T < 0$), v_+ must lag ϕ_- by a phase angle greater than a quarter but less than three-quarters of cycle. In a westerly shear ($U_T > 0$), on the other hand, it requires that v_+ either leads or lags ϕ_- by a phase difference less than one-quarter of cycle. Because v_+ leads the barotropic streamfunction ψ by a quarter cycle (Eq. 2.4), for unstable Rossby waves in an easterly shear, ψ leads ϕ_- by less than a half cycle. In a westerly shear, on the other hand, ψ lags ϕ_- by less than a half cycle. The conversion reaches maximum as the barotropic meridional wind is 180° out of phase with the thickness field in an easterly shear and precisely in phase in a westerly shear. For an unstable Rossby wave with a wavelength of 5000 km, the thickness perturbation leads (lags) barotropic meridional wind by more (less) than one-quarter wavelength in an easterly (westerly) shear (Fig. 3).

The energy conversion rates associated with an unstable Rossby wave are plotted in Fig. 4. The largest conversion of the mean potential energy to waves occurs at $y = \pm 1.5$, which is slightly poleward of the peak barotropic meridional wind but equatorward side of the peak temperature (Fig. 4a). The conversion between the eddy available potential energy to eddy baroclinic

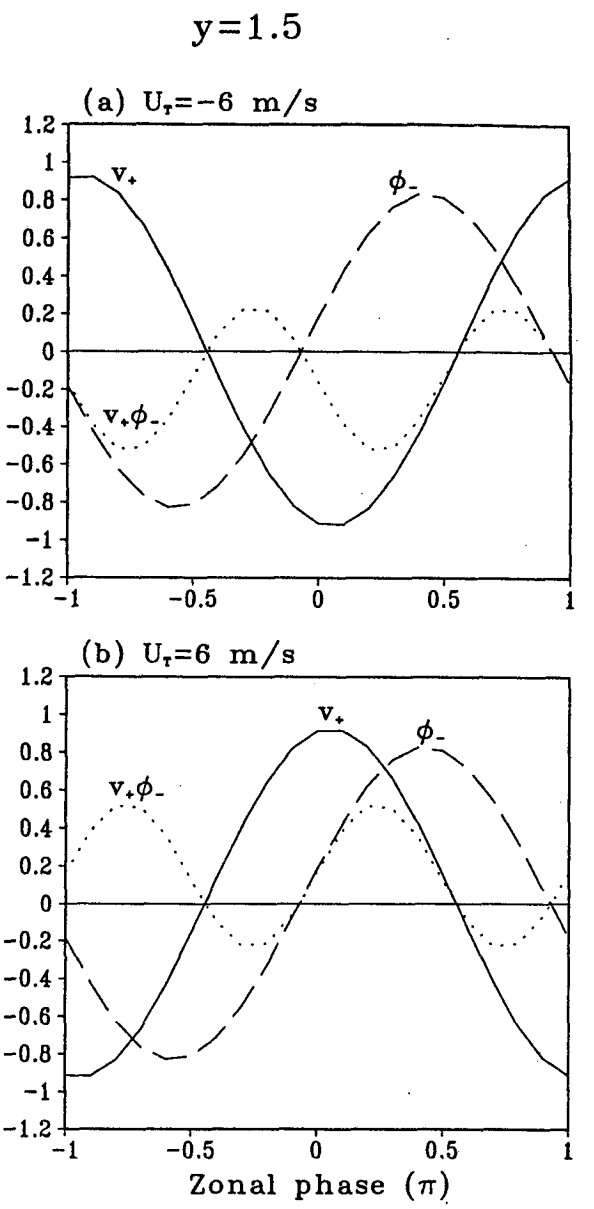

FIG. 3. Phases of temperature (dashed), barotropic meridional wind (solid), and their product (dotted) along $y = 1.5$ in (a) an easterly shear of $U_T = -6$ m s^{-1}, and (b) a westerly shear of $U_T = 6$ m s^{-1} for the $n = 1$ Rossby wave with a wavelength of 5000 km and heating coefficient $I = 0.8$.

kinetic energy is a source for amplification of the kinetic energy [see Eqs. (3.1) and (3.2)]. The conversion rate depends on the covariance between the thickness and wave-induced convergence [Eq. (3.4d)]. It also exhibits peaks at $y = \pm 1.5$ (Fig. 4b). The barotropic kinetic energy is primarily converted from the baroclinic kinetic energy, whereas direct generation of barotropic kinetic energy through baroclinic divergence acting on the vertical shear is much smaller [see Eq. (3.1)]. The conversion rate is proportional to the

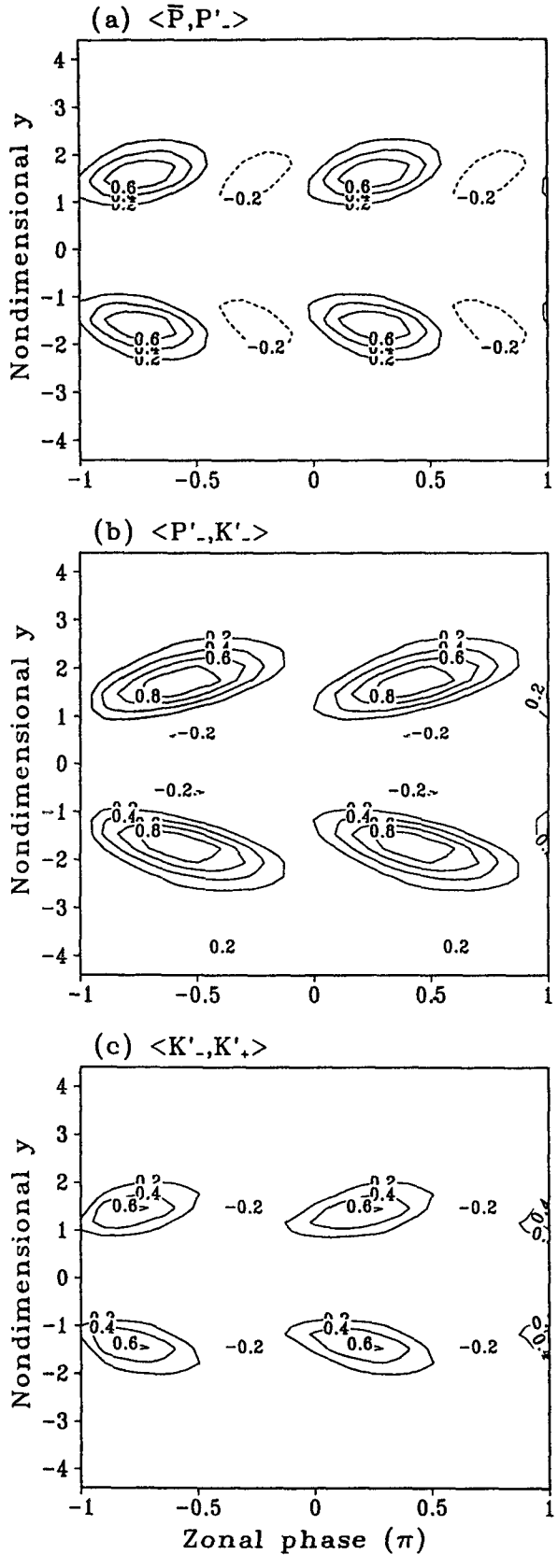

vertical shear and the inner product of the barotropic winds and zonal derivative of the baroclinic winds [Eq. (3.4e)]. Again, it maximizes at $y = \pm 1.5$ (Fig. 4c). In fact, all three energy conversion terms maximize at the latitudes where the geopotential extreme of the barotropic mode is located, implying the importance of the barotropic mode in the instability.

The vertical tilt of trough and ridge axes is against the direction of the vertical shear: eastward tilt with height in an easterly shear and westward tilt with height in a westerly shear (Fig. 5). This contrasts the vertical structure of stable Rossby waves that possess an equivalent barotropic structure in high latitudes and the upper and lower tropospheric perturbations are exactly 180° out of phase in the Tropics (WX96).

The energy cycle associated with unstable equatorial Rossby wave is shown by the schematics in Fig. 6 and implemented by the following description. Growing Rossby waves extract available potential energy from the mean flow. The condensational heating associated with wave-induced moisture convergence also contributes to the generation of wave available potential energy. The wave available potential energy then converts to the kinetic energy, driving the baroclinic wave motion. With the aid of vertical wind shear, the barotropic mode is excited by vertical mode interaction and gains kinetic energy from its baroclinic counterpart. Note that the barotropic motion can affect the conversion of wave available potential energy from mean flow to waves by changing the meridional heat flux. Amplification of perturbations depends on effective excitation of large-amplitude barotropic wave motions. The vertical shear plays essential roles in both the conversion from mean flow to wave available potential energy and the conversion from baroclinic to barotropic kinetic energy.

Other modes with the gravest meridional index such as westward propagating Yanai waves can also be destabilized by vertical shear but growth rate is much smaller than the $n = 1$ Rossby waves. In Part I, it was shown that the barotropic response is significant only for rotational waves but not for divergent Kelvin waves. Thus, Kelvin waves are baroclinically stable because of their inefficiency in the extraction of mean flow available potential energy.

5. Tropical Rossby wave instability versus midlatitude baroclinic instability

In this section, we examine the differences and similarities between the midlatitude baroclinic instability

FIG. 4. Energy conversions associated with the Rossby wave ($n = 1$) in an easterly shear of $U_T = -6$ m s^{-1} and $I = 0.8$: (a) from mean potential energy to eddy available potential energy, (b) from eddy available potential energy to baroclinic kinetic energy, and (c) from baroclinic kinetic energy to barotropic kinetic energy.

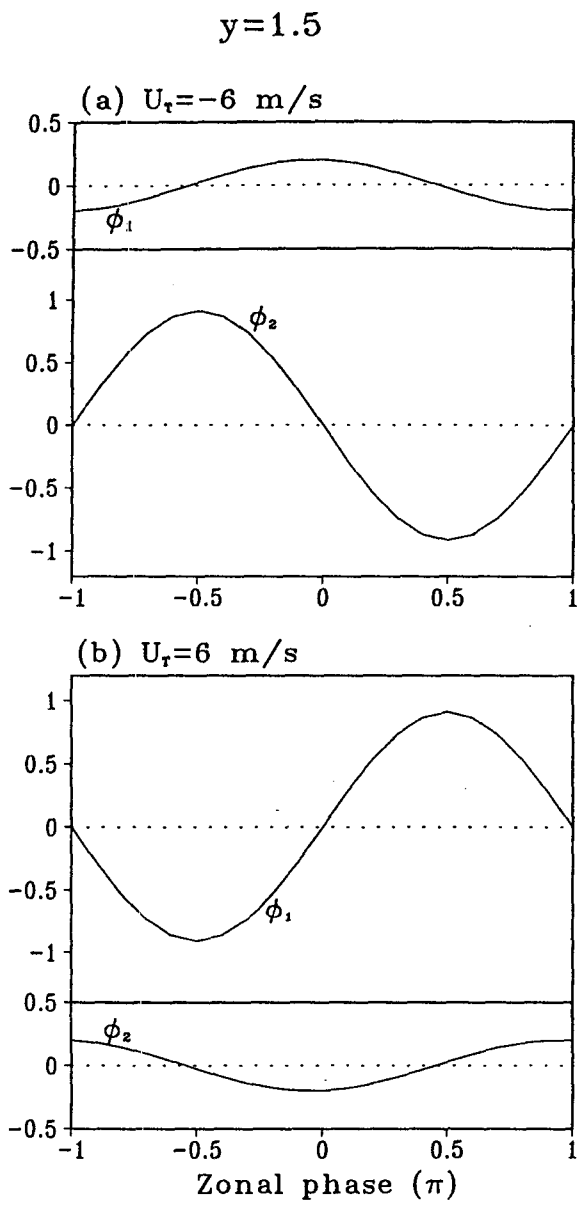

FIG. 5. Geopotential perturbation along $y = 1.5$ in the upper and lower troposphere with (a) an easterly shear ($U_T = -6$ m s^{-1}), and (b) a westerly shear ($U_T = 6$ m s^{-1}) for the $n = 1$ Rossby wave with a wavelength of 5000 km and heating coefficient $I = 0.8$.

and the tropical moist Rossby wave instability. For convenience of comparison, we introduce barotropic and baroclinic streamfunctions

$$\psi_m = (\psi_1' + \psi_2')/2, \quad \psi_T = (\psi_1' - \psi_2')/2, \quad (5.1)$$

where ψ_1' and ψ_2' are streamfunction at the upper and lower tropospheric levels, respectively. Adopting Phillips' two-level model (Holton 1994), the governing equations for inviscid, quasigeostrophic perturbation motion with a constant vertical shear on a midlatitude β plane are

$$\frac{D}{Dt}\nabla^2\psi_m + \beta\frac{\partial\psi_m}{\partial x} + U_T\frac{\partial}{\partial x}\nabla^2\psi_T = 0, \quad (5.2a)$$

$$\frac{D}{Dt}(\nabla^2\psi_T - 2\lambda^2\psi_T) + \beta\frac{\partial\psi_T}{\partial x} + U_T\frac{\partial}{\partial x}(\nabla^2\psi_m + 2\lambda^2\psi_m) = 0, \quad (5.2b)$$

where $\lambda^2 = f_0^2/(\sigma\Delta p^2)$; f_0 is the Coriolis parameter at a reference latitude; and σ is the static stability parameter. Typical parameter values are $f_0 = 1 \times 10^{-4}$ s^{-1}, $\sigma = 2 \times 10^{-6}$ m^2 s^{-2} Pa^{-2}, and $\Delta p = 500$ hPa.

The governing equations for the barotropic perturbation motion are similar for the quasigeostrophic baroclinic instability and the equatorial Rossby wave instability. In fact, Eq. (5.2a) is the same as Eq. (2.5) if the vertical shear is constant, except that the latter includes an extra term associated with divergence of the baroclinic mode. This suggests that the nature of the barotropic wave motion is the same for tropical and midlatitude Rossby waves. However, the equations for the baroclinic motion differ between the two types of waves. The midlatitude baroclinic motion is quasigeostrophic, whereas the equatorial baroclinic Rossby wave contains significant ageostrophic component.

Figure 7 shows the horizontal structure of an unstable midlatitude baroclinic wave in a zonal flow with westerly vertical shear (which is normal in midlatitude). The structure differs from that of an unstable tropical moist Rossby wave in several notable aspects. We have shown in section 4 that in order to convert the available potential energy from the basic flow to waves, the phases of geopotential and wind of the unstable tropical Rossby wave must tilt eastward with increasing latitudes. Unlike the unstable tropical Rossby waves, the phase shift between the barotropic and baroclinic modes is not latitude-dependent for the midlatitude baroclinic wave, thus the wave does not exhibit any meridional tilt. In addition, the barotropic mode is much stronger than the baroclinic mode. Another notable difference from the tropical Rossby wave is that the wind perturbation is dominantly meridional whereas the zonal wind anomaly tends to be weak. The differences in the structure between the unstable tropical and midlatitude Rossby waves result from the different nature of the baroclinic mode, because the excitation mechanism of the barotropic motion is essentially the same.

There are similarities between unstable midlatitude and equatorial Rossby waves. For instance, an easterly (westerly) shear confines the unstable perturbation in the lower (upper) troposphere. The constant phase lines of the unstable waves exhibit a vertical tilt against the direction of vertical shear: eastward (westward) tilt with height in easterly (westerly) shear. The barotropic meridional wind is nearly in phase with the temperature field such that the meridional heat flux acting on the

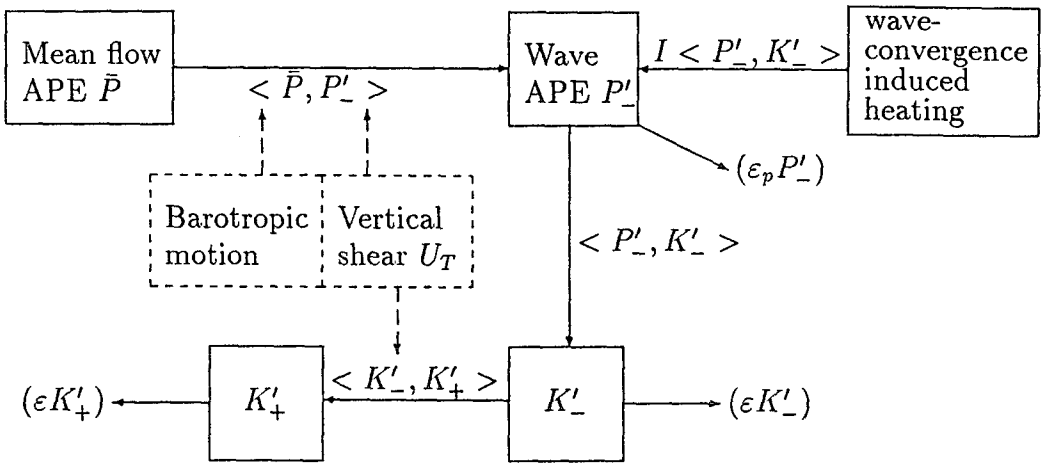

FIG. 6. Energy cycle associated with unstable equatorial Rossby waves.

vertical shear tends to intensify the perturbation motions.

The energy cycle for the tropical Rossby wave instability is somewhat similar to that of midlatitude baroclinic instability in the sense that $\langle \bar{P}, P'_- \rangle$ is a primary energy source for the perturbation growth. There are, however, major differences. First, strong vertical shear in higher latitudes implies large meridional temperature gradients of the basic state, whereas in the Tropics meridional temperature gradient can be weak although vertical shear is large, because of the smallness of the Coriolis parameter. As a consequence, in the midlatitudes, the advection of the basic state temperature by the perturbation meridional wind acts to intensify the perturbation thickness field for developing disturbances (Holton 1994). In the Tropics, however, the thermal advection tends to be small due to weak meridional gradient of the basic state temperature. Second, unstable tropical Rossby waves require that the ridge and tough axes tilt eastward with increasing latitude in order to change the quadrature relationship between v_+ and ϕ_- of the stable Rossby waves. In contrast, the developing midlatitude baroclinic wave does not have horizontally tilted trough and ridge axes.

It should also be pointed out that the midlatitude baroclinic instability does not require the presence of β effect [e.g., in an Eady (1949) model]—that is, the midlatitude baroclinic waves are essentially independent of planetary vorticity gradient. On the other hand, the tropical baroclinic unstable waves are modified Rossby waves for which the β effect is essential.

6. Impacts of meridional variation of the vertical shear

In the previous analysis (sections 4 and 5), we neglected meridional variation of the vertical shear. Observed mean flow vertical shear, however, exhibits considerable meridional variation in summer monsoon regions. In this section, we assess the effects of meridional variation of the vertical shear on the moist Rossby wave instability.

a. Tropical vertical shear

Easterly vertical shears in the Eastern Hemisphere are confined to the tropical region. To identify the effects of such a meridionally confined tropical vertical shear, we designed an ideal profile, which is shown in Fig. 8a. This shear profile is barotropically stable.

With such a wind shear, the growth rate is substantially reduced (Fig. 9). The instability occurs only if the nondimensional heating coefficient I is sufficiently large. The adiabatic equatorial Rossby waves are normally stable even when the shear is unrealistically large. For diabatic equatorial Rossby waves, the growth rate depends on wavelength and vertical shear in a similar manner as that for a constant shear (Fig. 1).

The reduced growth rate can be explained in terms of eddy energy generation, which is affected by horizontal wave structures. With strong meridional variation of the mean zonal flow, the baroclinic rotational waves are more tightly trapped near the equator (Fig. 10a). This was shown by Wilson and Mak (1984). In WX96, we also demonstrated that two barotropically stable meridional shears, with double westerly jets, tend to tightly trap equatorial waves with short wavelengths. When vertical shear is confined to the deep Tropics, the baroclinic mode is much more tightly trapped near the equator (between $y = -2$ and $y = 2$) with the strongest geopotential perturbation located at about one Rossby radius of deformation (Fig. 10a). The amplitude of zonal wind perturbation near the equator is enhanced compared with that in a constant shear. The barotropic mode tends to emanate to higher latitudes and tilts westward with latitude (Fig. 10b),

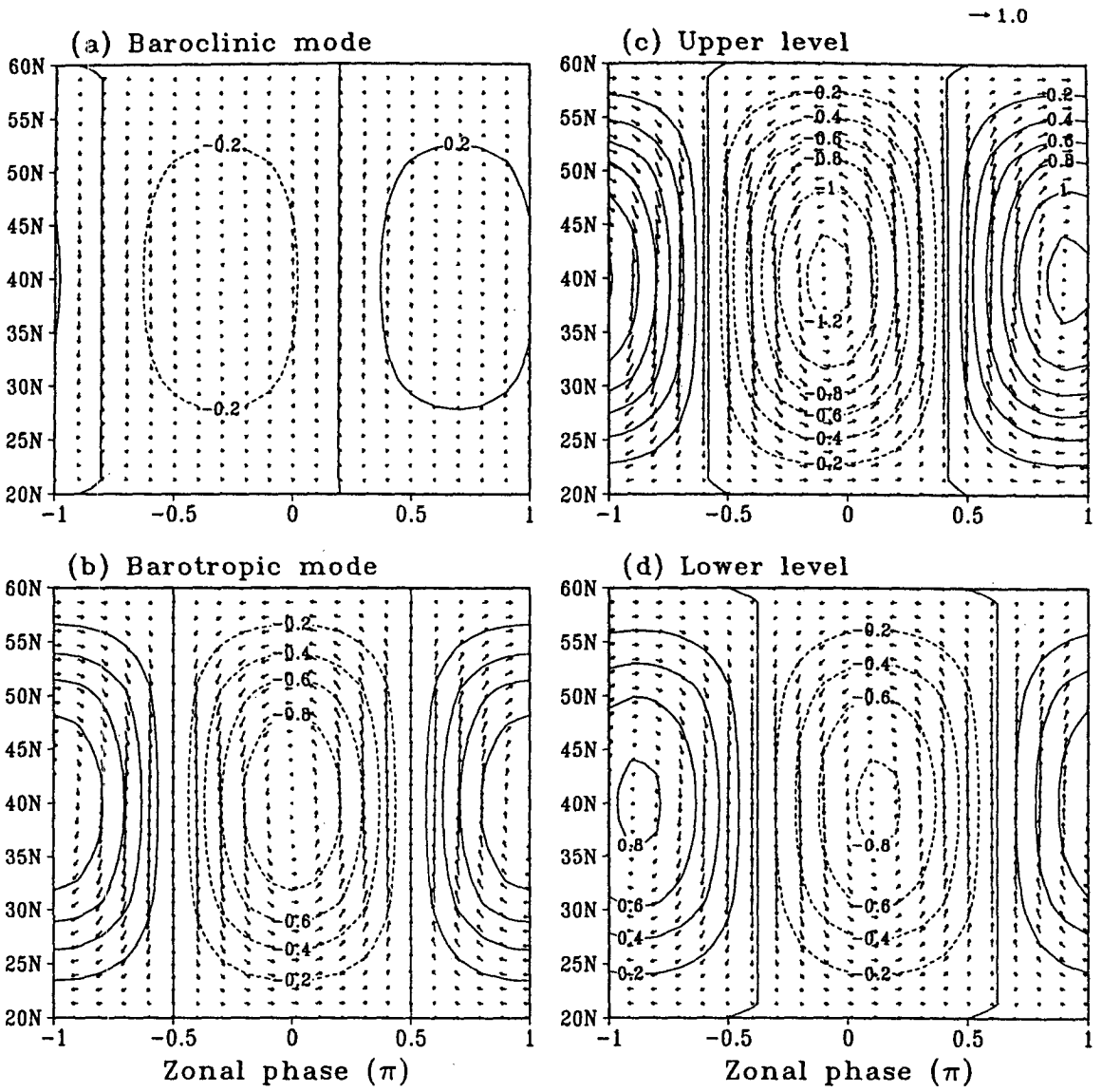

FIG. 7. As in Fig. 2 except for the midlatitude baroclinic wave with a wavelength of 4000 km and a vertical shear of $U_T = 10$ m s^{-1}.

just opposite to that in a constant shear. In correspondence with the changes in unstable wave structure, the energy conversion regions are closer to the equator (Fig. 11); all three energy conversion regions are now concentrated around one Rossby radius of deformation (Fig. 11).

The conversion rate of the mean to eddy available potential energy is proportional to the Coriolis parameter (Eq. 3.4f). The trapping of the waves by meridional shear thus reduces $\langle \bar{P}, P'_\perp \rangle$ and inhibits the baroclinic instability. The effect of vertical shear on tropical waves investigated by Kuo (1978) was combined with a barotropically unstable basic flow. The trapping effect of a barotropically unstable meridional shear is even stronger. Therefore, as the vertical shear is combined with a strong latitudinal shear that is close to the equator, the baroclinic instability virtually disappears. However, provided the latitudinal shear is not too strong and cumulus heating is present, the moist baroclinic instability remains possible.

b. Asymmetric vertical shear relative to the equator

During the northern summer, westward-moving disturbances are primarily observed north of the equator over the western Pacific and Indian monsoon regions. The large-scale vertical shear in the monsoon region is also asymmetric about the equator with strongest east-

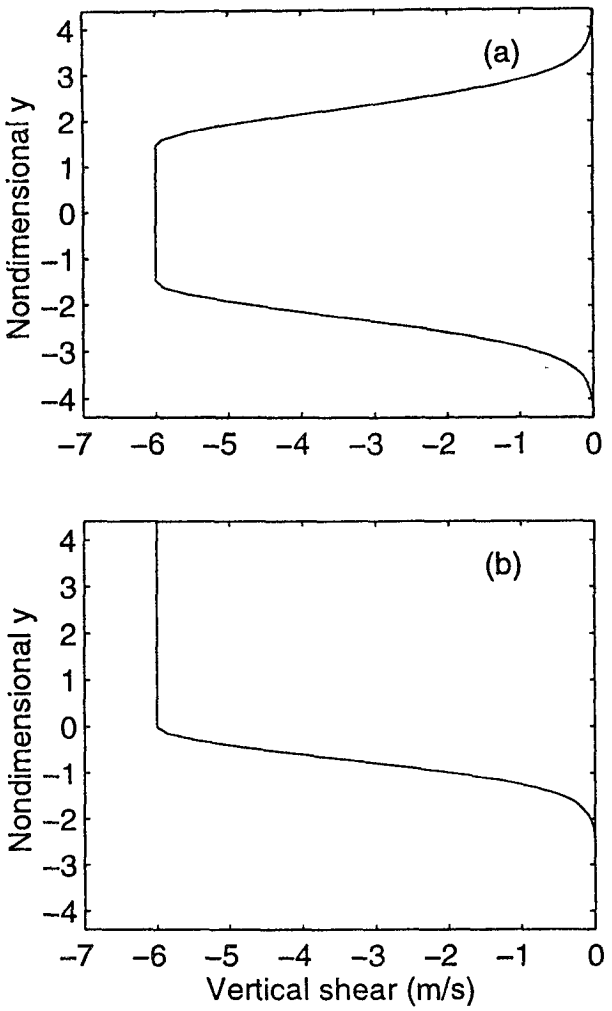

FIG. 8. Profiles of (a) a tropical wind shear, and (b) an asymmetric (relative to the equator) vertical shear.

erly shear locating at the Northern Hemisphere. To explore whether this hemispheric asymmetry in westward propagating low-frequency disturbances can partially be attributed to the influence of asymmetric distribution of the vertical shear, we consider a shear profile that has a constant amplitude of $U_T = -6$ m s^{-1} in the Northern Hemisphere but exponentially decays to zero at $y = -2$ (Fig. 8b).

With this asymmetric vertical shear distribution, perturbation motions at both the upper and lower troposphere are mainly confined to the Northern Hemisphere, whereas their magnitudes in the Southern Hemisphere are substantially suppressed (Fig. 12). The structure in the Northern Hemisphere resembles that obtained in the constant shear case. Zonal wind perturbation in the vicinity of the equator weakens considerably. Major energy conversion is accomplished between one and two Rossby radii of deformation in the Northern Hemisphere, where the vertical shear is prominent and the perturbations obtain large amplitude. It appears that the wave amplifies "locally" where the wave energy is generated. Because the wave energy generation [Eq. (3.4f)] depends on the vertical shear, the development of the unstable waves is, to a large degree, controlled by the meridional distribution of the vertical shear.

This experiment demonstrates that although free equatorial Rossby waves with the gravest meridional index are symmetric about the equator, the presence of the asymmetric (with respect to the equator) vertical shear can fundamentally alter the wave structure: localizing the unstable Rossby wave to the regions where the vertical shear is large. This provides a plausible explanation to the observed seasonal dependence of the asymmetric distribution of the westward-moving low-frequency disturbances.

7. Critical role of the planetary boundary layer on Rossby wave instability

Tropical boundary-layer flows interact with free atmospheric circulation and underlying sea surface temperature, playing a critical role in coupling collective effects of cumulus heating and equatorial dynamics (Wang and Li 1994). We now consider the effects of an Ekman boundary layer on moist Rossby wave instability. With an Ekman boundary layer, the model equations and vertical boundary conditions are slightly modified. They, along with energy equations, are given in the appendix.

Figure 13 compares the growth rates for $n = 1$ equatorial Rossby waves in zonal flows with an easterly and a westerly shear, respectively. For convenience of comparison, the growth rate obtained without boundary layer but with the same magnitude of the vertical shear is also given in Fig. 13. Without boundary layer effects the Rossby wave instability is independent of the sign of the vertical shear. With the effects of the boundary layer the growth rate becomes extremely sensitive to the sign of the vertical shear. A notable increase of the growth rate in an easterly shear is observed for wavelengths longer than 5000 km or shorter than 3000 km. For Rossby waves with wavelengths of 3000 to 5000 km the impact is moderate. On the other hand, the instability is virtually suppressed by the boundary layer effects for all wavelengths in a westerly shear.

What causes the asymmetry of the instability with respect to the direction of vertical shears? Examination of wave structures and energetics in the two different shears provides a clue. Similar to the case without a boundary layer, an easterly shear confines large perturbations to the lower troposphere (Figs. 14a,b). This results in a strong Ekman vertical velocity (Fig. 14c), which is determined by the lower-tropospheric geopotential perturbation and the boundary layer properties [Eq. (A2)]. Furthermore, the Ekman ver-

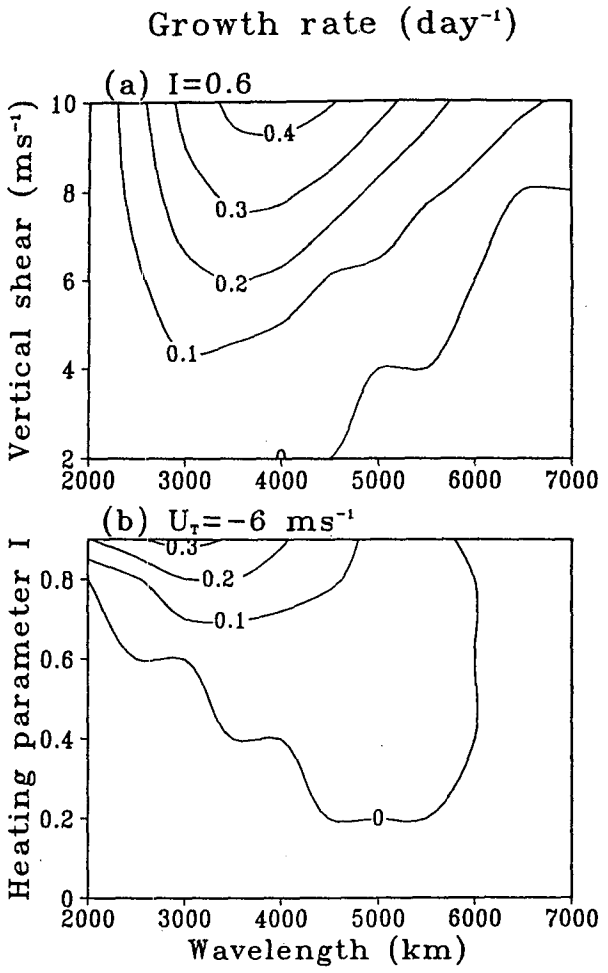

FIG. 9. (a) As in Fig. 1b except for a shear of Fig. 8a with different strength, and (b) growth rate as a function of wavelength and nondimensional heating parameter I with a shear of Fig. 8a.

tical velocity displays an in-phase relationship with both the lower-tropospheric geopotential and temperature perturbations (Figs. 14c,d). The generation of eddy available potential energy depends on the covariance between the surface friction-induced moisture convergence and the thickness field [Eq. (A3b)]. Therefore, the condensational heating due to the boundary layer moisture convergence contributes to amplification of the Rossby wave in an easterly shear. In addition, the barotropic meridional wind v_+ and the thickness ϕ_- have a similar phase relationship with that without a boundary layer such that the potential energy of the basic state can be converted to eddies. In contrast, a westerly shear confines large perturbation with semigeostrophic flow in the upper troposphere (Fig. 15a). In the lower troposphere, the geopotential perturbation is weak between $y = -1.5$ and $y = 1.5$ (Fig. 15b). The lower-tropospheric geopotential distribution results in weak and relatively small meridional scale for Ekman pumping velocity (Fig. 15c). As a consequence, the energy generation through the boundary layer moisture convergence is small. Although the baroclinic modes resemble each other in both shears, the excited barotropic modes differ. In a westerly shear, v_+ and ϕ_- are approximately in quadrature (Fig. 15d) such that the zonal average of the meridional heat flux is nearly zero. Therefore, the moist Rossby wave instability is not favored in a westerly shear.

8. Summary

The equatorial Rossby waves with gravest meridional structure are shown to be unstable when the vertical

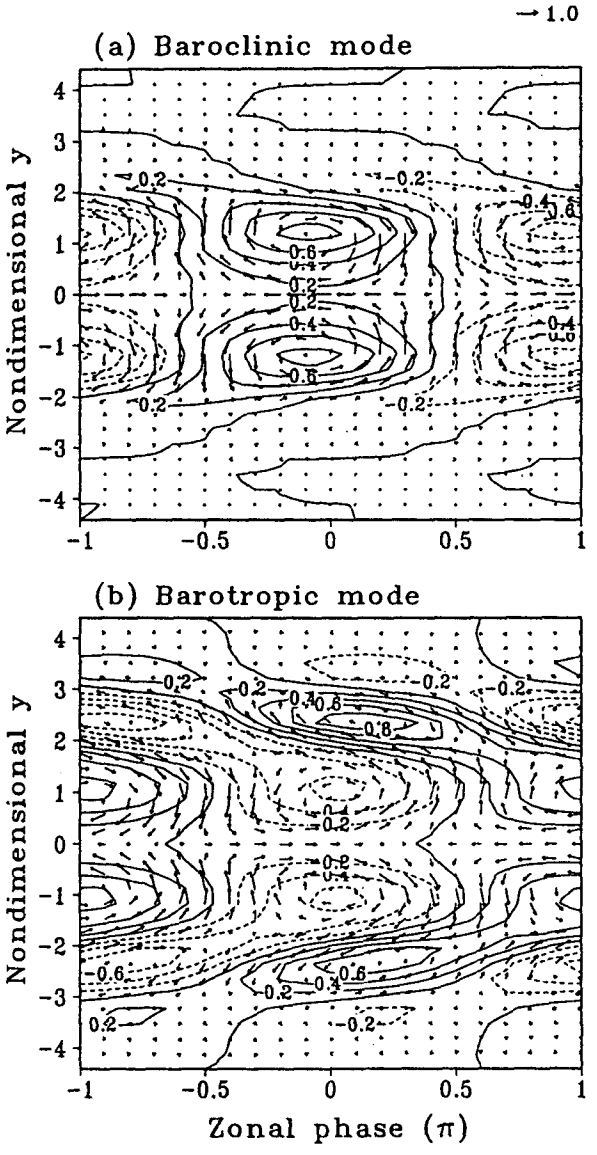

FIG. 10. (a) As in Fig. 2a and (b) as in Fig. 2b, except for a shear of Fig. 8a.

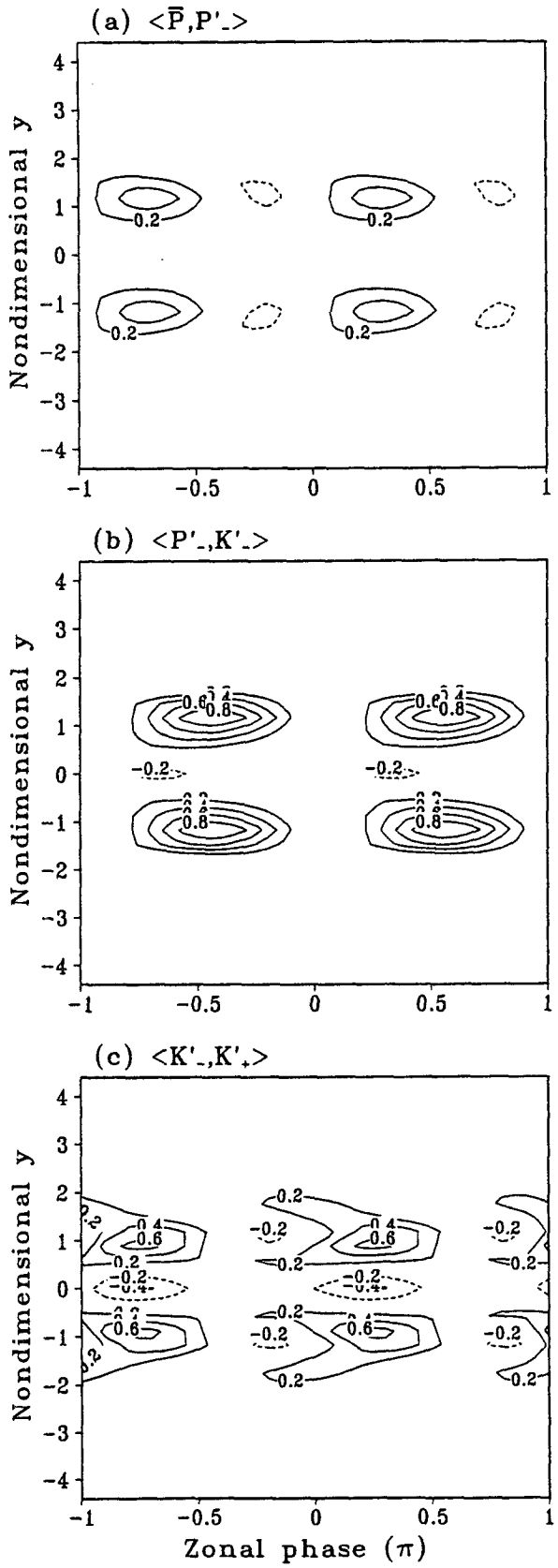

shear of the mean zonal flow exceeds certain critical value. Although the growth rate does not depend on the sign of the vertical shear, the vertical structure of the unstable waves does: Easterly (westerly) shears confine the unstable waves in the lower (upper) troposphere. For given strength of vertical shear and heating intensity there exists a most unstable wave. The preferred unstable wavelength increases with increasing vertical shear and decreases with increasing heating intensity, ranging typically from 3000 to 5000 km.

There are a number of distinct characteristics in the structure of the unstable equatorial Rossby waves compared with their stable counterparts: (a) the constant phase lines exhibit an eastward tilt with latitude; (b) there is no meridional emanation toward the extratropics; both the baroclinic and barotropic modes remain trapped at the equator, displaying a single peak in each hemisphere in the geopotential and meridional winds, while the temperature field is less trapped than its counterpart of a stable wave; and (c) the constant phase lines tilt with height against the direction of the vertical shear.

Such a wave structure favors the perturbations to extract available potential energy from the basic flow, because the conversion rate is proportional to the Coriolis parameter (latitude), vertical shear, and the covariance between temperature (thickness) and barotropic meridional wind. The horizontal tilt of the ridges and troughs of the unstable wave ensures that the temperature field leads (lags) the barotropic meridional wind by more (less) than a quarter wavelength in an easterly (westerly) shear. This warrants a conversion of mean flow energy to the waves. In contrast, for a stable Rossby wave the temperature is precisely in quadrature with barotropic meridional wind so that no energy is transferred from mean flow to eddy.

The present study suggests that vertical wind shears have profound influences on the instability of equatorial rotational waves. The instability mechanism selects only those westward propagating rotational waves, because transfer of the mean potential energy requires significant barotropic motion, which is excited by zonal stretch of vorticity associated with baroclinic motion acting on the vertical shear of the basic flow (WX96). The barotropic mode is rotational in nature, therefore, resonant barotropic motion can only be excited by the westward propagating rotational waves but not by the eastward propagating divergent Kelvin waves. In this regard, baroclinic instability is a mechanism through which a tropical westward propagating rotational wave can be destabilized, whereas eastward propagating waves cannot.

The meridional variations of vertical shear have significant influences on the moist Rossby waves. When

FIG. 11. As in Fig. 4 except for the vertical shear shown in Fig. 8a.

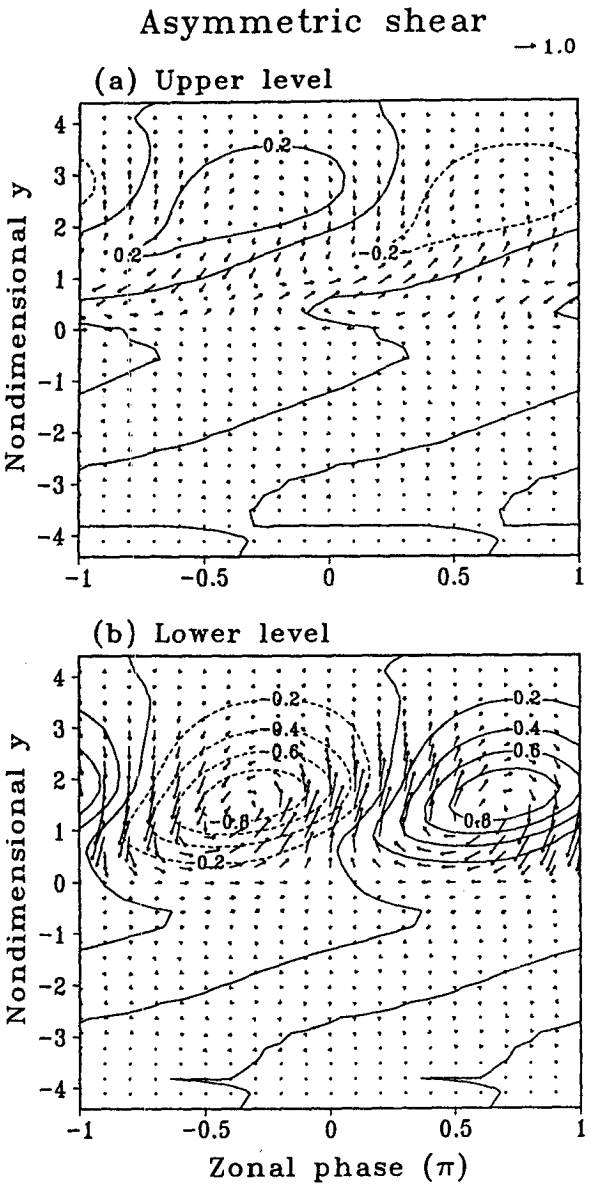

FIG. 12. (a) As in Fig. 2c, and (b) as in Fig. 2d, except for a shear of Fig. 8b.

the vertical shear is suppressed south of the equator, the unstable Rossby waves are strongly asymmetric with respect to the equator and large perturbations are confined to the Northern Hemisphere where the vertical shear is prominent. If a vertical shear is confined to the Tropics, the instability is much weaker than that in a meridionally invariant vertical shear. Structure of unstable waves in a tropical vertical shear differs dramatically from that in a constant shear, especially the barotropic component. To have the mean potential energy transfer to eddies, that is, $U_T\overline{yv_+\phi_-} > 0$, both the baroclinic and barotropic components should have large amplitude sufficiently far away from the equator. Strong meridional shear of the mean zonal wind causes tight trapping of the rotational waves near the equator and does not favor baroclinic instability in the Tropics.

In the presence of an Ekman boundary layer, the tropical Rossby wave instability is more favorable in an easterly shear than in a westerly shear due to a combined effect of boundary layer Ekman pumping and vertical shear. The asymmetric tropical moist Rossby wave instability with respect to the sign of vertical shear is attributed to the differences in the wave structure and surface friction-induced moisture convergence. First, in an easterly (westerly) shear, the phase shift between the barotropic meridional wind and the thickness favors (unfavors) the conversion of potential energy from the mean flow to eddies. Second, the frictional moisture convergence in an easterly shear has larger contribution to the generation of eddy available potential energy than in a westerly shear, because easterly (westerly) shears trap perturbations in the lower (upper) troposphere, inducing stronger (weaker) Ekman pumping.

The destabilization of moist Rossby waves by regional easterly vertical shears has important implication. During the northern summer season, large easterly shears exist over the Indian monsoon and western North Pacific regions. It provides a favorable large-scale environment for westward propagating moist Rossby wave disturbances to develop only north of the equator. The tropical Rossby waves have two energy sources: vertical shear of the mean zonal flow via baroclinic instability and the surface friction-induced moisture convergence. Both processes contribute to the de-

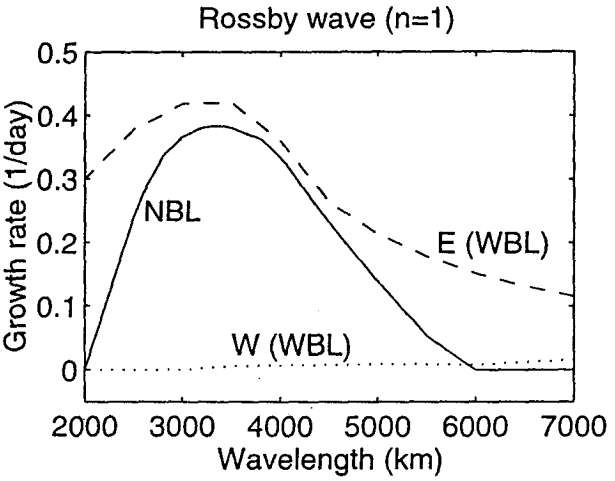

FIG. 13. Growth rate for the Rossby wave ($n = 1$) with an Ekman boundary layer in an easterly shear of $U_T = -6$ m s^{-1} (dashed) and a westerly shear of $U_T = 6$ m s^{-1} (dotted), compared with that without a boundary layer (solid). Nondimensional heating parameters associated with the wave convergence and the boundary layer frictional convergence are $I = 0.6$ and $B = 1.6$, respectively.

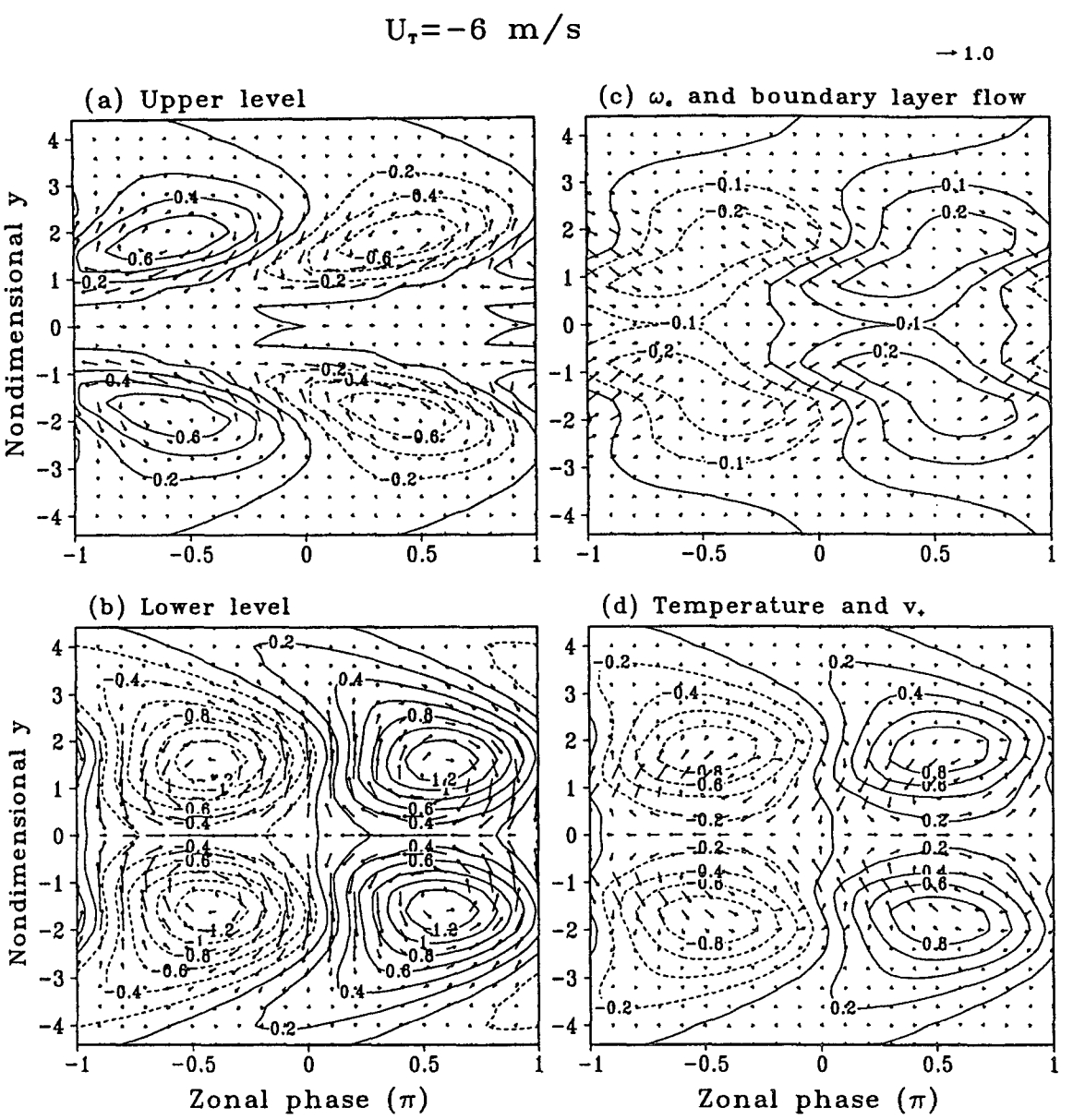

FIG. 14. Geopotential and flow patterns of the $n = 1$ Rossby wave with a wavelength of 5000 km in an easterly shear of $U_T = -6$ m s^{-1} at the (a) upper troposphere, and (b) lower troposphere. (c) Vertical velocity at the top of the boundary layer, and (d) baroclinic geopotential and barotropic wind.

velopment of tropical Rossby waves. The disturbances take the form of asymmetric tropical Rossby waves modified by convective heating. The most unstable Rossby waves predicted by the model compare favorably to the observed vorticity waves (Lau and Lau 1990) in their horizontal and vertical structures, preferred wavelength and propagation speed, and their seasonality.

It should be pointed out that although the present study is based on an equatorial β-plane model, its qualitative validity is confirmed by an analogous study using a spherical coordinate model. Furthermore, the present study is the first step to perceive how the realistic basic state regulates the intraseasonal disturbances. The impacts of more complicated three-dimensional monsoon mean flows on the low-frequency disturbances during the boreal summer will be reported in a separate paper (Wang and Xie 1996, manuscript submitted to *J. Atmos. Sci.*).

Acknowledgments. The authors thank Prof. Peter Webster, who made a thorough review and pointed out

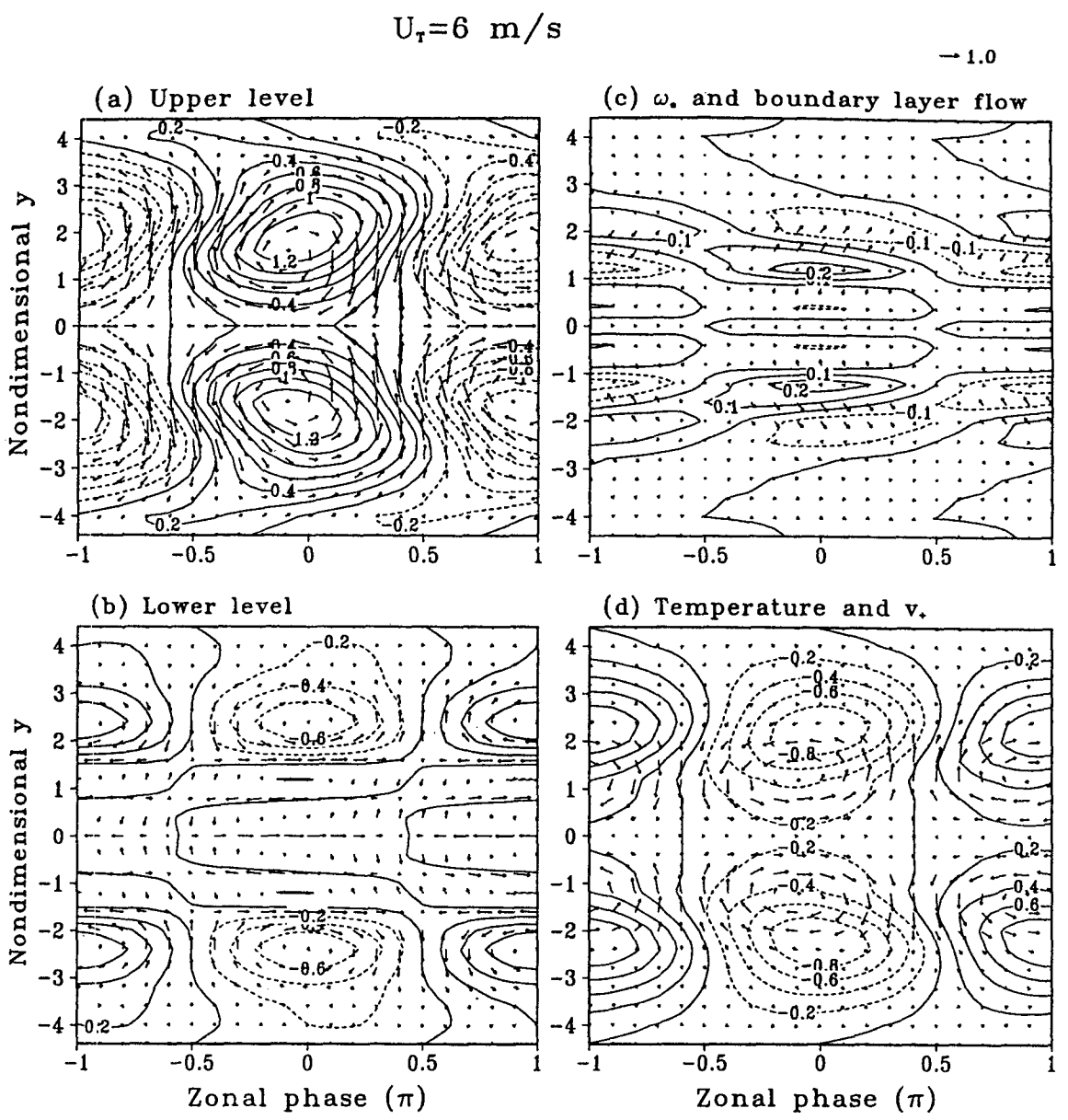

FIG. 15. As in Fig. 14 except for a westerly shear of $U_T = 6$ m s^{-1}.

a few errors in a previous version of the manuscript. This research is supported by the Climate Dynamics Program of the National Science Foundation under Grant ATM 94-00759. This is the School of Ocean and Earth Science and Technology publication number 4129.

APPENDIX

Governing Equations with Boundary Layer

Let us consider a barotropic frictional boundary layer following Wang and Rui (1990b). The counterpart of Eq. (2.2) for a constant shear becomes

$$\frac{Du_+}{Dt} - yv_+ + \frac{\partial \phi_+}{\partial x} = -2U_T\frac{\partial u_-}{\partial x} - U_T\frac{\partial v_-}{\partial y} + 4U_T\omega_e - \epsilon u_+, \quad \text{(A.1a)}$$

$$\frac{Dv_+}{Dt} + yu_+ + \frac{\partial \phi_+}{\partial y} = -U_T\frac{\partial v_-}{\partial x} - \epsilon v_+, \quad \text{(A.1b)}$$

$$\frac{\partial u_+}{\partial x} + \frac{\partial v_+}{\partial y} = 0, \quad \text{(A.1c)}$$

$$\frac{Du_-}{Dt} - yv_- + \frac{\partial \phi_-}{\partial x} = -U_T\frac{\partial u_+}{\partial x} - \epsilon u_-, \quad \text{(A.1d)}$$

$$\frac{Dv_-}{Dt} + yu_- + \frac{\partial \phi_-}{\partial y} = -U_T \frac{\partial v_+}{\partial x} - \epsilon v_-, \quad \text{(A.1e)}$$

$$\frac{D\phi_-}{Dt} + (1 - I)\left(\frac{\partial u_-}{\partial x} + \frac{\partial v_-}{\partial y}\right) = (B - 1)\omega_e + yU_T v_+ - \epsilon_p \phi_-, \quad \text{(A.1f)}$$

where ω_e is vertical pressure velocity at the top of the boundary layer p_e. In the derivation of Eqs. (A.1a–f), an upper boundary condition $\omega_0 = \omega_e$ was assumed for convenience of deriving energy equations. Wang and Rui (1990b) showed that this boundary condition leads to similar results with those using a rigid-lid condition. The Ekman pumping vertical velocity at the bottom of the free atmosphere p_e is expressed as (Wang and Rui 1990b)

$$\omega_e = \frac{(p_s - p_e)}{2\Delta p(E^2 + y^2)}\left[\frac{2y}{E^2 + y^2}\left(E\frac{\partial}{\partial y} - y\frac{\partial}{\partial x}\right) - E\left(\frac{\partial^2}{\partial x^2} + \frac{\partial^2}{\partial y^2}\right) + \frac{\partial}{\partial x}\right]\phi_e, \quad \text{(A.2)}$$

where E is a nondimensional Ekman number; ϕ_e is geopotential at p_e, which is approximated by $\phi_2 = \phi_+ - \phi_-$.

The nondimensional number B measures condensational heating due to vertical motion at the top of the boundary layer. Typical value of B can be estimated in terms of the static stability parameter of the basic state and the moisture content in the boundary layer (Wang 1988). In this analysis, we assume $I = 0.6$, $B = 1.6$, $p_s = 1000$ hPa, $p_e = 950$ hPa, $\Delta p = 425$ hPa, and a damping scale of the boundary layer friction is one-third day.

Energy equations can be derived from (A.1), which have forms similar to Eqs. (3.1–3.3), except that an additional term (GK_e) appears on the rhs of the barotropic kinetic energy equation (3.1) and an additional term (GP) on the rhs of the wave potential energy equation (3.3). Here, GK_e and GP are

$$GK_e = 4U_T\overline{u_+\omega_e}, \quad \text{(A.3a)}$$

$$GP = (B - 1)\overline{\omega_e\phi_-}. \quad \text{(A.3b)}$$

Here, GK_e denotes the generation of barotropic kinetic energy caused by the coupling of the barotropic mode and the planetary boundary layer via vertical shear. Here, GP is associated with a net effect of generation of eddy available potential energy due to latent heating associated with boundary layer frictional moisture convergence and energy depletion caused by boundary layer dissipation.

REFERENCES

Cadet, D. L., 1983: The monsoon over the Indian Ocean during summer 1975. Part II: Break and active monsoons. *Mon. Wea. Rev.*, **111,** 95–108.

Eady, E. T., 1949: Long waves and cyclone waves. *Tellus,* **1,** 33–52.

Holton, J. R., 1994: *An Introduction to Dynamic Meteorology.* 3d ed. Academic Press, 391 pp.

Kuo, H.-L., 1978: A two-level model study of the combined barotropic and baroclinic instability in the Tropics. *J. Atmos. Sci.,* **35,** 1840–1859.

Lau, K.-H., and N.-C. Lau, 1990: Observed structure and propagation characteristics of tropical summer time synoptic scale disturbances. *Mon. Wea. Rev.,* **118,** 1888–1913.

Lau, K.-M., and L. Peng, 1990: Origin of low frequency (intraseasonal) oscillations in the tropical atmosphere. Part III: Monsoon dynamics. *J. Atmos. Sci.,* **47,** 1443–1462.

Murakami, T., 1980: Empirical orthogonal function analysis of satellite-observed outgoing longwave radiation during summer. *Mon. Wea. Rev.,* **108,** 205–222.

Nitta, T., 1987: Convective activities in the western Pacific and their impact on the Northern Hemisphere summer circulation. *J. Meteor. Soc. Japan,* **65,** 373–390.

Wang, B., 1988: Dynamics of tropical low-frequency waves: An analysis of the moist Kelvin wave. *J. Atmos. Sci.,* **45,** 2051–2065.

——, and H. Rui, 1990a: Synoptic climatology of transient tropical intraseasonal convection anomalies: 1975–1985. *Meteor. Atmos. Phys.,* **44,** 43–61.

——, and ——, 1990b: Dynamics of the coupled moist Kelvin–Rossby wave on an equatorial beta-plane. *J. Atmos. Sci.,* **47,** 397–413.

——, and T. Li, 1994: Convective interaction with boundary-layer dynamics in the development of a tropical intraseasonal system. *J. Atmos. Sci.,* **51,** 1386–1400.

——, and X. Xie, 1996a: Low-frequency equatorial waves in vertically sheared zonal flow. Part I: Stable waves. *J. Atmos. Sci.,* **53,** 449–467.

——, and ——, 1996b: On the impacts of Northern Hemisphere summer monsoon on intraseasonal oscillation. *J. Atmos. Sci.*

Wilson, J. D., and M. K. Mak, 1984: Tropical response to lateral forcing with a latitudinally and zonally nonuniform basic state. *J. Atmos. Sci.,* **41,** 1187–1201.

Zhang, M., and M. A. Geller, 1994: Selective excitation of tropical atmospheric waves in wave-CISK: The effect of vertical wind shear. *J. Atmos. Sci.,* **51,** 353–368.